



The Applicability of the New General Mathematical Equation for Buckling and Post-buckling Analysis of Biaxially Loaded Thin Rectangular Plates with Free Edge

^{1*} Edubi, H.U., ² Adah, E.I., & ³ Ubi, S.U.

¹Department of Civil Engineering, Faculty of Engineering, University of Cross River, Nigeria
hycienthedubi@gmail.com

²Department of Civil and Environmental Engineering, Faculty of Engineering, University of Calabar, Nigeria
edwardadah@unical.edu.ng

³Department of Civil Engineering, Faculty of Engineering, University of Cross River, Nigeria
emmaubi2015@yahoo.com

*Corresponding Author: Edubi, Hycienth; hycienthedubi@gmail.com

Manuscript History

Received: 08/09/2025

Revised: 18/01/2026

Accepted: 19/01/2026

Published: 17/02/2026

<https://doi.org/10.5281/zenodo.18736039>

Abstract: Thin rectangular plates, widely used in engineering structures such as bridges, aircraft, and ships, are highly susceptible to nonlinear buckling under biaxial compressive loading and large deflections, where classical linear theories fail to provide accurate predictions. This study applies a new general biaxial buckling equation under large deflections to six plate configurations with one free edge, deriving unique equations for each. The Ritz energy method with polynomial shape functions was employed to evaluate bending and membrane stiffness characteristics. These stiffness values were substituted into the general equation to obtain specific equations for the configurations: SSFS (simply supported–simply supported–free–simply supported), SCFS (simply supported–clamped–free–simply supported), CSFS (clamped–simply supported–free–simply supported), CCFS (clamped–clamped–free–simply supported), SCFC (simply supported–clamped–free–clamped), and CCFC (clamped–clamped–free–clamped) under biaxial compression. The proposed models are versatile, applicable to both uniaxial and biaxial loading under small and large deflection conditions. Comparisons of predicted critical loads of SSFS (15.415), SCFS (26.472), CSFS (19.283), CCFS (29.891), SCFC (47.451), and CCFC (50.714) with published results show minimal percentage differences within acceptable limits. Findings reveal that the biaxial buckling load coefficient decreases with increasing biaxial load ratio, while decreasing aspect ratio reduces the buckling load. Thus, the general biaxial buckling equation for large deflections is validated as applicable and suitable for analyzing these plates.

Keywords: Large Deflection, Biaxial Buckling, Shape Function, Free Edge, Rectangular Plate

INTRODUCTION

The A thin rectangular plate is a structural element with a flat, right-angled geometry whose thickness is much smaller than its length and width (Megson, 2013). It is widely used in engineering to support and transmit compressive forces (Zhang & Zhang, 2013). These plates can operate either as standalone structural components for example, bridge deck slabs and floor panels or as integrated elements within more complex assemblies, such as aircraft wings, and ship hulls etc. (Hassan & Saeed, 2024). Owing to their relatively small thickness compared

to their other dimensions, thin plates possess a high slenderness ratio, which, while enabling material efficiency and weight reduction, also makes them inherently susceptible to buckling when subjected to compressive loads (Brighenti, 2005; Kubiak, 2013). Buckling is a critical instability phenomenon in which the plate undergoes sudden lateral deformation, often well before reaching its ultimate material strength (Jones, 2006; Jerath, 2020). This mode of failure is particularly significant in thin plates because it can result in a rapid loss of load-carrying capacity, potentially leading to partial or total structural collapse (Li et al., 2019; Zhang & Tan, 2023; Barsotti, 2024). The prediction, prevention, and control of buckling in thin plates are therefore essential aspects of structural design, requiring advanced analytical, numerical, and experimental approaches to ensure safety, reliability, and serviceability in engineering applications (Bai, 2003; Carrera et al., 2011; Giuseppe & Matteo, 2017).

While extensive research has been conducted on uniaxial buckling of plates, the phenomenon of biaxial buckling particularly under conditions of large displacements remains comparatively less explored and understood (Ibearugbulem et al., 2020; Adah et al., 2023). Large displacements introduce geometric nonlinearity into the plate's response, fundamentally altering its structural behaviour and challenging the applicability of classical analytical models like the widely used Kirchhoff plate theory (Szilard, 2004; Chandel et al., 2020). When deflections become large, the assumptions by classical plate theory break down, and can yield significant inaccuracies in estimating critical loads and deformation patterns (Ugural, 2017). In such cases, a more comprehensive theoretical framework is required that accounts for nonlinear membrane forces arising from in-plane deformations of the middle surface. The von Kármán plate theory offers such a solution, as it incorporates both bending and stretching effects (Altenbach, 2020). This approach enables a more realistic representation of plate behaviour under large deflections, thereby improving the accuracy of buckling load predictions and deformation analysis in practical engineering applications where large-displacement effects cannot be neglected (Yue et al., 2017). However, it requires rigorous analytical and computational effort to obtain a solution (Dai et al., 2014; Bilbao et al., 2015; Zhong & Liao, 2018). The primary aim of this research is to apply the new general mathematical equation developed by Adah and Edubi (2025) to developed the different new expressions Postbuckling analysis of thin rectangular plates with a free edge under large deflection. To achieve this, Polynomial displacement shape functions are applied to determine the stiffness characteristics of six thin rectangular plates with free edges, namely SSFS (simply supported - simply supported - free - simply supported), SCFS (simply supported - clamped - free - simply supported), CSFS (clamped - simply supported - free - simply supported), CCFS (clamped - clamped - free - simply supported), SCFC (simply supported - clamped - free - clamped), and CCFC (clamped - clamped - free - clamped). Furthermore, the stiffnesses are apply on the general expression to obtained the postbuckling expression for each boundary condition for plates subjected to biaxial forces.

MATERIALS AND METHODS

The general biaxial buckling and postbuckling equation for thin rectangular plates is given by Edubi (2025) as

$$N_x = \eta_{LX} \frac{D}{a^2} \quad (2.1)$$

Where

$$\eta_{LX} = \frac{\left[\left(K_{bx} + \frac{2}{2^2} K_{bxy} + \frac{1}{2^4} K_{by} \right) + \frac{3}{2} \frac{1}{(h_{\max})^2} \left(\frac{w}{t} \right)^2 \left(K_{mx} + \frac{2}{2^2} K_{mxy} + \frac{k_{my}}{2^4} \right) \right]}{\left[K_{Nx} + \frac{nK_{Ny}}{2^2} \right]} \quad (2.2)$$

Equation (2.2) is the Biaxial Buckling and postbuckling Load coefficient equation of thin rectangular plates under large deflection.

Where,

$$k_{bx} = \int_0^1 \int_0^1 \left(\frac{\partial^2 h_R}{\partial R^2} \times h_Q \right)^2 dRdQ \quad (2.3)$$

$$k_{bxy} = \int_0^1 \int_0^1 \left(\frac{\partial h_R}{\partial R} \times \frac{\partial h_Q}{\partial Q} \right)^2 dRdQ \quad (2.4)$$

$$k_{by} = \int_0^1 \int_0^1 \left(h_R \times \frac{\partial^2 h}{\partial Q^2} \right)^2 dRdQ \quad (2.5)$$

$$k_{mx} = \int_0^1 \int_0^1 \left(\frac{\partial h_R}{\partial R} \times h_Q \right)^4 dRdQ \quad (2.6)$$

$$k_{mxy} = \int_0^1 \int_0^1 \left(\frac{\partial h_R}{\partial R} \times h_Q \right)^2 \left(h_R \times \frac{\partial h_Q}{\partial Q} \right)^2 dRdQ \quad (2.7)$$

$$k_{my} = \int_0^1 \int_0^1 \left(h_R \times \frac{\partial h_Q}{\partial Q} \right)^4 dRdQ \quad (2.8)$$

$$k_{Nx} = \int_0^1 \int_0^1 \left(\frac{\partial h_R}{\partial R} \times h_Q \right)^2 dRdQ \quad (2.9)$$

$$k_{Nxy} = \int_0^1 \int_0^1 \left(\frac{\partial h_R}{\partial R} \times h_Q \right) \left(h_R \times \frac{\partial h_Q}{\partial Q} \right) dRdQ \quad (2.10)$$

$$k_{Ny} = \int_0^1 \int_0^1 \left(h_R \times \frac{\partial h_Q}{\partial Q} \right)^2 dRdQ \quad (2.11)$$

$$\mathbf{n} = \frac{\mathbf{N}_y}{\mathbf{N}_x} \quad \text{is the Load factor} \quad (2.12)$$

$$\mathcal{Z} = \frac{b}{a} \quad \text{is the aspect ratio} \quad (2.13)$$

w = deflected function and

t = the thickness of the plate.

D = flexural rigidity of the plate

2.1 Stiffness Evaluation

To determine the stiffness values, the deflected shape profile for each plate condition is required. The general polynomial deflected shape function for thin rectangular plates is given as

$$w = Ah \quad (2.15)$$

$$h = \frac{w}{A} \quad (2.16)$$

The shape profiles h is given in the [Table-1](#)

Table-1 The Polynomial Displacement Shape Profile of Plates with Free Edge ([Ibearugbulem et al., 2014](#))

S/N	Plate Type	Shape Function $w = Ah$ Shape Profile, h
1	CSFS	$(R - 2R^3 + R^4)(2.8Q^2 - 5.2Q^3 + 3.8Q^4 - Q^5)$
2	SSFS	$(R - 2R^3 + R^4) \left(\frac{7}{3}Q - \frac{10}{3}Q^3 + \frac{10}{3}Q^4 - Q^5 \right)$
3	SCFS	$(1.5R^2 - 2.5R^3 + R^4) \left(\frac{7}{3}Q - \frac{10}{3}Q^3 + \frac{10}{3}Q^4 - Q^5 \right)$
4	CCFS	$(1.5R^2 - 2.5R^3 + R^4)(2.8Q^2 - 5.2Q^3 + 3.8Q^4 - Q^5)$
5	SCFC	$(R^2 - 2R^3 + R^4) \left(\frac{7}{3}Q - \frac{10}{3}Q^3 + \frac{10}{3}Q^4 - Q^5 \right)$
6	CCFC	$(R^2 - 2R^3 + R^4)(2.8Q^2 - 5.2Q^3 + 3.8Q^4 - Q^5)$

2.2 Stiffnesses for CSFS Plate

The shape function for CSFS plate is given by

$$h = (R - 2R^3 + R^4)(2.8Q^2 - 5.2Q^3 + 3.8Q^4 - Q^5) \quad (2.17)$$

$$\text{Let, } h = h_R \times h_Q \quad (2.18)$$

Where, $h_R = (R - 2R^3 + R^4)$ and $h_Q = (2.8Q^2 - 5.2Q^3 + 3.8Q^4 - Q^5)$

To obtain the stiffness, partial derivatives and necessary expansion of the stiffnesses in Equations (2.3) to (2.11) gives

$$\begin{aligned} K_{bx} &= \int_0^1 \int_0^1 \left(\frac{\partial^2 h_R}{\partial R^2} \times h_Q \right)^2 dRdQ \\ &= \int_0^1 \int_0^1 (144R^2 - 288R^3 + 144R^4) \\ &\quad \times (7.84Q^4 - 29.12Q^5 + 48.32Q^6 - 45.12Q^7 + 24.84Q^8 - 7.6Q^9 + Q^{10}) dRdQ \\ &= \left[\frac{144}{3} - \frac{288}{4} + \frac{144}{5} \right] \times \left[\frac{7.84}{5} - \frac{29.12}{6} + \frac{48.32}{7} - \frac{45.12}{8} + \frac{24.84}{9} - \frac{7.6}{10} + \frac{1}{11} \right] \\ &= \left(\frac{24}{5} \right) \left(\frac{1976}{28875} \right) \\ K_{bx} &= 0.3284779221 \end{aligned} \quad (2.19)$$

$$\begin{aligned} K_{bxy} &= \int_0^1 \int_0^1 \left(\frac{\partial h_R}{\partial R} \times \frac{\partial h_Q}{\partial Q} \right)^2 dRdQ \\ &= \int_0^1 \int_0^1 (1 - 12R^2 + 8R^3 + 36R^4 - 48R^5 + 16R^6) \\ &\quad \times (31.36Q^2 - 174.72Q^3 + 413.6Q^4 - 530.24Q^5 + 387.04Q^6 - 152Q^7 + 25Q^8) dRdQ \\ &= \left[1 - \frac{12}{3} + \frac{8}{4} + \frac{36}{5} - \frac{48}{6} + \frac{16}{7} \right] \times \left[\frac{31.36}{3} - \frac{174.72}{4} + \frac{413.6}{5} - \frac{530.24}{6} + \frac{387.04}{7} - \frac{152}{8} + \frac{25}{9} \right] \\ &= \left(\frac{17}{35} \right) \left(\frac{298}{1575} \right) \\ K_{bxy} &= 0.0919002268 \end{aligned} \quad (2.20)$$

$$\begin{aligned} K_{by} &= \int_0^1 \int_0^1 \left(h_R \times \frac{\partial^2 h_Q}{\partial Q^2} \right)^2 dRdQ \\ &= \int_0^1 \int_0^1 (R^2 - 4R^4 + 2R^5 + 4R^6 - 4R^7 + R^8) \\ &\quad \times (31.36 - 349.44Q + 1484.16Q^2 - 3069.44Q^3 + 3327.36Q^4 - 1824Q^5 + 400Q^6) dRdQ \\ &= \left[\frac{1}{3} - \frac{4}{5} + \frac{2}{6} + \frac{4}{7} - \frac{4}{8} + \frac{1}{9} \right] \times \left[31.36 + \frac{349.44}{2} + \frac{1484.16}{3} - \frac{3069.44}{4} + \frac{3327.36}{5} - \frac{1824}{6} + \frac{400}{7} \right] \\ &= \left(\frac{31}{630} \right) \left(\frac{2288}{875} \right) \\ K_{by} &= 0.1286675737 \end{aligned} \quad (2.21)$$

$$\begin{aligned} K_{Nx} &= \int_0^1 \int_0^1 \left(\frac{\partial h_R}{\partial R} \times h_Q \right)^2 dRdQ \\ &= \int_0^1 \int_0^1 (1 - 12R^2 - 8R^3 + 36R^4 - 48R^5 + 16R^6) \\ &\quad \times (7.84Q^4 - 29.12Q^5 + 48.32Q^6 - 45.12Q^7 + 24.84Q^8 - 7.6Q^9 + Q^{10}) dRdQ \\ &= \left[1 - \frac{12}{3} + \frac{8}{4} + \frac{36}{5} - \frac{48}{6} + \frac{16}{7} \right] \times \left[\frac{7.84}{5} - \frac{29.12}{6} + \frac{48.32}{7} - \frac{45.12}{8} + \frac{24.84}{9} - \frac{7.6}{10} + \frac{1}{11} \right] \\ &= \left(\frac{17}{35} \right) \left(\frac{1976}{28875} \right) \\ K_{Nx} &= 0.0332388374 \end{aligned} \quad (2.22)$$

$$K_{Nxy} = \int_0^1 \int_0^1 \left(\frac{\partial h_R}{\partial R} \times h_Q \right) \left(h_R \times \frac{\partial h_Q}{\partial Q} \right) dRdQ$$

$$\begin{aligned}
&= \int_0^1 \int_0^1 (R - 8R^3 + 5R^4 + 12R^5 - 14R^6 + 4R^7) \\
&\quad \times (15.68Q^3 - 72.8Q^4 + 144.96Q^5 + 157.92Q^6 + 99.36Q^7 - 34.2Q^8 + 5Q^9) dRdQ \\
&= \left[\frac{1}{2} - \frac{8}{4} + \frac{5}{5} + \frac{12}{6} - \frac{14}{7} + \frac{4}{8} \right] \times \left[\frac{15.68}{4} - \frac{72.8}{5} + \frac{144.96}{6} - \frac{157.92}{7} + \frac{99.36}{8} - \frac{34.2}{9} + \frac{5}{10} \right] \\
K_{Nxy} &= (0) \left(\frac{2}{25} \right) = 0 \tag{2.23}
\end{aligned}$$

$$\begin{aligned}
K_{Ny} &= \int_0^1 \int_0^1 \left(h_R \times \frac{\partial h_Q}{\partial Q} \right)^2 dRdQ \\
&= \int_0^1 \int_0^1 (R^2 - 4R^4 + 2R^5 + 4R^6 - 4R^7 + R^8) \\
&\quad \times (31.36Q^2 - 174.72Q^3 + 413.6Q^4 - 530.24Q^5 + 387.04Q^6 - 152Q^7 + 25Q^8) dRdQ \\
&= \left[\frac{1}{3} - \frac{4}{5} + \frac{2}{6} + \frac{4}{7} - \frac{4}{8} + \frac{1}{9} \right] \times \left[\frac{31.36}{3} - \frac{174.72}{4} + \frac{413.6}{5} - \frac{530.24}{6} + \frac{387.04}{7} - \frac{152}{8} + \frac{25}{9} \right] \\
K_{Ny} &= \left(\frac{31}{630} \right) \left(\frac{298}{1575} \right) \\
K_{Ny} &= 0.0093101537 \tag{2.24}
\end{aligned}$$

$$\begin{aligned}
K_{mx} &= \int_0^1 \int_0^1 \left(\frac{\partial h_R}{\partial R} \times h_Q \right)^4 dRdQ \\
&= \int_0^1 \int_0^1 (1 - 24R^2 + 16R^3 + 216R^4 - 288R^5 - 768R^6 + 1728R^7 + 144R^8 - 3200R^9 + 3456R^{10} - 1536R^{11} \\
&\quad + 256R^{12})(61.4656Q^8 - 456.6016Q^9 + 1605.632Q^{10} - 3521.6384Q^{11} + 5352.1024Q^{12} \\
&\quad - 5926.2464Q^{13} + 4894.656Q^{14} - 3034.2656Q^{15} + 1399.4896Q^{16} - 467.808Q^{17} \\
&\quad + 107.44Q^{18} - 15.2Q^{19} + Q^{20}) dRdQ \\
&= \left[1 - \frac{24}{3} + \frac{16}{4} + \frac{216}{5} - \frac{288}{6} - \frac{768}{7} + \frac{1728}{8} + \frac{144}{9} - \frac{3200}{10} + \frac{3456}{11} - \frac{1536}{12} + \frac{256}{13} \right] \\
&\quad \times \left[\frac{61.4656}{9} - \frac{456.6016}{10} + \frac{1605.632}{11} - \frac{3521.6384}{12} + \frac{5352.1024}{13} - \frac{5926.2464}{14} \right. \\
&\quad \left. + \frac{4894.656}{15} Q^{14} - \frac{3034.2656}{16} + \frac{1399.4896}{17} - \frac{467.808}{18} + \frac{107.44}{19} - \frac{15.2}{20} Q^{19} + \frac{1}{21} \right] \\
K_{mx} &= 0.0027493343 \tag{2.25}
\end{aligned}$$

$$\begin{aligned}
K_{mxy} &= \int_0^1 \int_0^1 \left(\frac{\partial h_R}{\partial R} \times h_Q \right)^2 \left(h_R \times \frac{\partial h_Q}{\partial Q} \right)^2 dRdQ \\
&= \int_0^1 \int_0^1 (R^2 - 16R^4 + 10R^5 + 88R^6 - 108R^7 - 159R^8 + 344R^9 - 60R^{10} - 296R^{11} + 292R^{12} - 112R^{13} \\
&\quad + 16R^{14})(245.8624Q^6 - 2283.008Q^7 + 9845.7856Q^8 - 26058.5472Q^9 + 47122.4832Q^{10} \\
&\quad - 61323.4944Q^{11} + 58881.4976Q^{12} - 42025.1264Q^{13} + 22123.7376Q^{14} - 8375.424Q^{15} \\
&\quad + 2163.24Q^{16} - 342Q^{17} + 25Q^{18}) dRdQ \\
&= \left[\frac{1}{3} - \frac{16}{5} + \frac{10}{6} + \frac{88}{7} - \frac{108}{8} - \frac{159}{9} + \frac{344}{10} - \frac{60}{11} - \frac{296}{12} + \frac{292}{13} - \frac{112}{14} + \frac{16}{15} \right] \\
&\quad \times \left[\frac{245.8624}{7} - \frac{2283.008}{8} + \frac{9845.7856}{9} - \frac{26058.5472}{10} + \frac{47122.4832}{11} - \frac{61323.4944}{12} \right. \\
&\quad \left. + \frac{58881.4976}{13} - \frac{42025.1264}{14} + \frac{22123.7376}{15} - \frac{8375.424}{16} + \frac{2163.24}{17} - \frac{342}{18} + \frac{25}{19} \right] \\
K_{mxy} &= 0.0000920936 \tag{2.26}
\end{aligned}$$

$$K_{my} = \int_0^1 \int_0^1 \left(h_R \times \frac{\partial h_Q}{\partial Q} \right)^4 dRdQ$$

$$\begin{aligned}
&= \int_0^1 \int_0^1 (R^4 - 8R^6 + 4R^7 + 24R^8 - 24R^9 - 26R^{10} + 48R^{11} - 8R^{12} - 28R^{13} + 24R^{14} - 8R^{15} \\
&\quad + R^{16}) (983.4496Q^4 - 10958.4384Q^5 + 56468.0704Q^6 - 177785.0368Q^7 \\
&\quad + 380627.17444Q^8 - 583395.2256Q^9 + 655996.8256Q^{10} - 544919Q^{11} \\
&\quad + 331672.9216Q^{12} - 144172.16Q^{13} + 42456Q^{14} - 7600Q^{15} + 625Q^{16}) dRdQ \\
&= \left(\frac{1}{5} - \frac{8}{7} + \frac{4}{8} + \frac{24}{9} - \frac{24}{10} - \frac{26}{11} + \frac{48}{12} - \frac{8}{13} - \frac{28}{14} + \frac{24}{15} - \frac{8}{16} + \frac{1}{17} \right) \left(\frac{983.4496}{5} - \frac{10958.4384}{6} + \frac{56468.0704}{7} \right. \\
&\quad - \frac{177785.0368}{8} + \frac{380627.1744}{9} - \frac{583395.2256}{10} + \frac{655996.8256}{11} - \frac{544918.5792}{12} \\
&\quad \left. + \frac{331672.9216}{13} - \frac{144172.16}{14} + \frac{42456}{15} - \frac{7600}{16} + \frac{625}{17} \right) \tag{2.27}
\end{aligned}$$

$$K_{my} = 0.0001994590$$

In similar manner, the others plate boundary conditions were determined and the results of the stiffnesses are presented in Table 2.

2.3 Specific Equations

The stiffness values for each plate type in Table-2 together with h_{max} (at $R = 0.5$; $Q = 1$) were substituted into Equation (2.2) to obtain the new specific equations presented in Table-3. The selected values of the non-dimensional parameters R and Q represent the coordinates at which the maximum deflection of the plate occurs.

RESULTS AND DISCUSSION

The bending stiffness, external load stiffnesses and membrane stiffness of the rectangular plates studied as calculated using Equations (2.3) to (2.11) with their respective shape profile, and the results are presented in Table-2.

Table-2 Bending, External load, and Membrane Stiffnesses of Rectangular Plates with Free Edge

PLATE TYPE	K_{bx}	K_{bxy}	K_{by}	K_{Nx}	K_{Ny}	K_{mx}	K_{mxy}	K_{my}
SSFS	4.0257816258	1.0331065760	0.1874527589	0.4073707598	0.1046611237	0.3681508201	0.0100347190	0.0271358458
SCFS	1.5096681097	0.1823129252	0.0287226002	0.0718889576	0.0160367851	0.0127248132	0.0003322402	0.0007118745
CSFS	0.3284779221	0.0919002268	0.1286675737	0.0332388374	0.0093101537	0.0027493343	0.0000920936	0.0001994590
CCFS	0.1231792208	0.0162176871	0.0197151927	0.0058656772	0.0014265558	0.0000950284	0.0000030491	0.0000052326
SCFC	0.6709636043	0.0405139834	0.0060468632	0.0159753239	0.0033761653	0.0005451058	0.0000189513	0.0000343368
CCFC	0.0547463203	0.0036039305	0.0041505669	0.0013034838	0.0003003275	0.0000040708	0.0000001739	0.0000002524

Using the stiffnesses for these plates, the biaxial buckling load coefficient models were calculated using Equation (2.2) and with the values of h_{max} (at $R=0.5$; $Q=1$) the results are shown in Table-3.

Table-3 Expressions for Biaxial Buckling Load Coefficient of Thin Rectangular Plates with Free Edge Under Large Deflection

Plate Type	Biaxial Buckling Load Equation, $N_x = \eta_{Lx} \frac{D}{a^2}$
SSFS	$ \eta_{Lx} = \frac{\left[\left(K_{bx} + \frac{2}{2^2} K_{bxy} + \frac{1}{2^4} K_{by} \right) + \frac{3}{2} \frac{1}{(h_{max})^2} \left(\frac{w}{t} \right)^2 \left(K_{mx} + \frac{2}{2^2} K_{mxy} + \frac{k_{my}}{2^4} \right) \right]}{\left[K_{Nx} + \frac{nK_{Ny}}{2^2} \right]} $ $ \left[\left(4.0257816258 + \frac{2.0662131519}{2^2} + \frac{0.1874527589}{2^4} \right) + \left(\frac{w}{t} \right)^2 \left(3.1808230858 + \frac{0.1733999450}{2^2} + \frac{0.2344537074}{2^4} \right) \right] $ $ \left[0.4073707598 + \frac{0.1046611237n}{2^2} \right] $

SCFS	$\left[\left(1.5096681097 + \frac{0.3646258503}{2^2} + \frac{0.0287226002}{2^4} \right) + \left(\frac{w}{t} \right)^2 \left(0.6871399122 + \frac{0.0358819380}{2^2} + \frac{0.0384412218}{2^4} \right) \right]$
	$\left[0.0718889576 + \frac{0.0160367851n}{2^2} \right]$
CSFS	$\left[\left(0.3284779221 + \frac{0.1838004535}{2^2} + \frac{0.1286675737}{2^4} \right) + \left(\frac{w}{t} \right)^2 \left(0.2639360939 + \frac{0.0176819768}{2^2} + \frac{0.0191480601}{2^4} \right) \right]$
	$\left[0.0332388374 + \frac{0.0093101537n}{2^2} \right]$
CCFS	$\left[\left(0.1231792208 + \frac{0.0324353741}{2^2} + \frac{0.0197151927}{2^4} \right) + \left(\frac{w}{t} \right)^2 \left(0.0570170109 + \frac{0.0036589608}{2^2} + \frac{0.0031395316}{2^4} \right) \right]$
	$\left[0.0058656772 + \frac{0.0014265558n}{2^2} \right]$
SCFC	$\left[\left(0.6709636043 + \frac{0.0810279667}{2^2} + \frac{0.0060468632}{2^4} \right) + \left(\frac{w}{t} \right)^2 \left(0.1177428497 + \frac{0.0081869662}{2^2} + \frac{0.0074167388}{2^4} \right) \right]$
	$\left[0.0159753239 + \frac{0.0033761653n}{2^2} \right]$
CCFC	$\left[\left(0.0547463203 + \frac{0.0072078609}{2^2} + \frac{0.0041505669}{2^4} \right) + \left(\frac{w}{t} \right)^2 \left(0.0097699831 + \frac{0.0008348431}{2^2} + \frac{0.0006057322}{2^4} \right) \right]$
	$\left[0.0013034838 + \frac{0.0003003275n}{2^2} \right]$

The biaxial buckling Load coefficient, η_{Lx} for each of these rectangular plates with free edges were calculated for square plate condition where the aspect ratio is 1, with the deflection-to-thickness ratio ranging between 0 and 1 at interval of 0.1. The results are shown in Tables-4 to 9.

Table-4 Biaxial Buckling Load Coefficient for SSFS Plate with aspect ratio of 1.0

n	η_{Lx}											
	0	0.1	0.2	0.3	0.4	0.5	0.6	0.7	0.8	0.9	1	
w/t												
0	15.415	15.028	14.661	14.312	13.978	13.660	13.356	13.065	12.787	12.520	12.264	
0.1	15.503	15.114	14.745	14.393	14.058	13.738	13.432	13.140	12.860	12.591	12.334	
0.2	15.767	15.372	14.996	14.639	14.298	13.972	13.661	13.364	13.079	12.806	12.544	
0.3	16.207	15.801	15.415	15.048	14.697	14.362	14.043	13.737	13.444	13.164	12.895	
0.4	16.824	16.403	16.002	15.620	15.256	14.909	14.577	14.260	13.956	13.664	13.385	
0.5	17.617	17.176	16.756	16.356	15.975	15.611	15.264	14.932	14.613	14.308	14.016	
0.6	18.586	18.120	17.678	17.256	16.854	16.470	16.104	15.753	15.417	15.095	14.787	
0.7	19.731	19.237	18.767	18.319	17.892	17.485	17.096	16.724	16.367	16.026	15.698	
0.8	21.053	20.525	20.024	19.546	19.091	18.656	18.241	17.844	17.463	17.099	16.749	
0.9	22.550	21.985	21.448	20.936	20.449	19.983	19.538	19.113	18.706	18.315	17.941	
1	24.224	23.617	23.040	22.490	21.966	21.466	20.989	20.531	20.094	19.675	19.272	

Table-5 Biaxial Buckling Load Coefficient for SCFS Plate with aspect ratio of 1.0

n	η_{Lx}											
	0	0.1	0.2	0.3	0.4	0.5	0.6	0.7	0.8	0.9	1	
w/t												
0	26.472	25.894	25.341	24.811	24.303	23.815	23.347	22.896	22.463	22.046	21.643	
0.1	26.578	25.998	25.442	24.910	24.400	23.911	23.440	22.988	22.553	22.134	21.730	
0.2	26.895	26.308	25.747	25.208	24.692	24.196	23.720	23.263	22.822	22.398	21.990	

0.3	27.425	26.826	26.254	25.705	25.178	24.673	24.188	23.721	23.272	22.839	22.423
0.4	28.166	27.552	26.963	26.400	25.859	25.340	24.841	24.362	23.901	23.457	23.029
0.5	29.120	28.484	27.876	27.293	26.734	26.198	25.682	25.187	24.710	24.251	23.809
0.6	30.285	29.624	28.991	28.385	27.804	27.246	26.710	26.194	25.699	25.221	24.761
0.7	31.662	30.971	30.310	29.676	29.068	28.485	27.924	27.385	26.867	26.368	25.887
0.8	33.251	32.525	31.830	31.165	30.527	29.914	29.326	28.760	28.215	27.691	27.186
0.9	35.051	34.286	33.554	32.853	32.180	31.534	30.914	30.317	29.743	29.191	28.658
1	37.064	36.255	35.481	34.739	34.028	33.345	32.689	32.058	31.451	30.867	30.304

Table-6 Biaxial Buckling Load Coefficient for CSFS Plate with aspect ratio of 1.0

n	η_{Lx}										
	0	0.1	0.2	0.3	0.4	0.5	0.6	0.7	0.8	0.9	1
w/t											
0	19.283	18.758	18.260	17.788	17.340	16.914	16.509	16.122	15.753	15.401	15.064
0.1	19.374	18.846	18.346	17.872	17.422	16.994	16.586	16.198	15.827	15.473	15.134
0.2	19.645	19.110	18.603	18.122	17.666	17.232	16.818	16.425	16.049	15.690	15.346
0.3	20.097	19.550	19.031	18.540	18.073	17.629	17.206	16.803	16.418	16.051	15.700
0.4	20.731	20.166	19.631	19.124	18.642	18.184	17.748	17.332	16.936	16.557	16.195
0.5	21.545	20.958	20.402	19.875	19.374	18.898	18.445	18.013	17.601	17.207	16.831
0.6	22.541	21.926	21.345	20.793	20.270	19.772	19.297	18.846	18.414	18.002	17.608
0.7	23.717	23.071	22.459	21.878	21.327	20.803	20.305	19.829	19.375	18.942	18.527
0.8	25.074	24.391	23.744	23.131	22.548	21.994	21.467	20.964	20.484	20.026	19.588
0.9	26.612	25.887	25.201	24.550	23.931	23.343	22.783	22.250	21.741	21.254	20.789
1	28.332	27.560	26.829	26.136	25.477	24.851	24.255	23.687	23.145	22.628	22.132

Table-7 Biaxial Buckling Load Coefficient for CCFS Plate with aspect ratio of 1.0

n	η_{Lx}										
	0	0.1	0.2	0.3	0.4	0.5	0.6	0.7	0.8	0.9	1
w/t											
0	29.891	29.181	28.504	27.858	27.241	26.650	26.084	25.542	25.022	24.523	24.043
0.1	30.000	29.287	28.608	27.960	27.340	26.747	26.179	25.635	25.113	24.612	24.131
0.2	30.326	29.606	28.919	28.264	27.637	27.038	26.464	25.914	25.387	24.880	24.393
0.3	30.870	30.137	29.438	28.771	28.133	27.523	26.939	26.379	25.842	25.326	24.831
0.4	31.632	30.880	30.164	29.481	28.827	28.202	27.604	27.030	26.480	25.951	25.444
0.5	32.611	31.836	31.098	30.393	29.720	29.075	28.458	27.867	27.299	26.755	26.231
0.6	33.807	33.005	32.239	31.509	30.810	30.142	29.502	28.889	28.301	27.736	27.194
0.7	35.222	34.385	33.588	32.827	32.099	31.403	30.737	30.098	29.485	28.897	28.331

0.8	36.854	35.979	35.144	34.348	33.586	32.858	32.161	31.492	30.851	30.236	29.644
0.9	38.703	37.784	36.908	36.071	35.272	34.507	33.775	33.073	32.399	31.753	31.132
1	40.770	39.802	38.879	37.998	37.156	36.350	35.579	34.839	34.130	33.449	32.795

Table-8 Biaxial Buckling Load Coefficient for SCFC Plate with aspect ratio of 1.0

n	η_{Lx}										
	0	0.1	0.2	0.3	0.4	0.5	0.6	0.7	0.8	0.9	1
w/t											
0	47.451	46.469	45.526	44.622	43.752	42.916	42.111	41.336	40.588	39.868	39.172
0.1	47.534	46.550	45.606	44.700	43.829	42.991	42.185	41.408	40.660	39.938	39.241
0.2	47.784	46.796	45.847	44.936	44.060	43.218	42.407	41.626	40.874	40.148	39.448
0.3	48.202	47.204	46.247	45.328	44.445	43.595	42.778	41.990	41.231	40.499	39.792
0.4	48.786	47.776	46.808	45.877	44.983	44.124	43.296	42.499	41.731	40.990	40.275
0.5	49.537	48.512	47.528	46.584	45.676	44.803	43.963	43.153	42.373	41.621	40.895
0.6	50.456	49.411	48.409	47.447	46.523	45.634	44.778	43.953	43.159	42.392	41.653
0.7	51.541	50.474	49.450	48.468	47.523	46.615	45.741	44.899	44.087	43.304	42.549
0.8	52.793	51.700	50.652	49.645	48.678	47.747	46.852	45.989	45.158	44.356	43.582
0.9	54.212	53.090	52.013	50.980	49.986	49.031	48.111	47.225	46.372	45.548	44.754
1	55.798	54.643	53.535	52.471	51.448	50.465	49.519	48.607	47.728	46.881	46.063

Table-9 Biaxial Buckling Load Coefficient for CCFC Plate with aspect ratio of 1.0

n	η_{Lx}										
	0	0.1	0.2	0.3	0.4	0.5	0.6	0.7	0.8	0.9	1
w/t											
0	50.714	49.572	48.480	47.435	46.434	45.475	44.555	43.671	42.821	42.004	41.217
0.1	50.800	49.656	48.562	47.516	46.513	45.552	44.630	43.745	42.894	42.075	41.287
0.2	51.058	49.908	48.809	47.757	46.749	45.784	44.857	43.967	43.111	42.289	41.497
0.3	51.488	50.328	49.220	48.159	47.143	46.169	45.235	44.337	43.475	42.645	41.846
0.4	52.090	50.917	49.795	48.722	47.694	46.709	45.764	44.856	43.983	43.144	42.336
0.5	52.864	51.673	50.535	49.446	48.403	47.403	46.444	45.522	44.636	43.785	42.965
0.6	53.810	52.598	51.440	50.331	49.269	48.251	47.275	46.337	45.435	44.568	43.734
0.7	54.928	53.691	52.508	51.377	50.293	49.254	48.257	47.300	46.379	45.494	44.642
0.8	56.218	54.952	53.742	52.584	51.474	50.411	49.390	48.410	47.469	46.563	45.691
0.9	57.680	56.381	55.139	53.951	52.813	51.722	50.675	49.669	48.703	47.774	46.879
1	59.314	57.979	56.702	55.480	54.309	53.187	52.110	51.077	50.083	49.127	48.207

Tables-4 to 9 present the biaxial buckling load coefficients for rectangular plates with SSFS, SCFS, CSFS, CCFS, SCFC, and CCFC boundary conditions. It is observed that as deflection increases, the biaxial buckling load coefficient increases, while as the applied biaxial load increases, the corresponding buckling load coefficient decreases. This trend is consistent across all plate configurations considered in this study. To validate the adequacy of these models, the undeformed state (where the deflection-to-thickness ratio, $w/t = 0$) of the buckling load coefficient for these rectangular plates when subjected to uniaxial compressive force (where the biaxial buckling ratio, $n = N_y/N_x = 0$) is compared with the readily available results by Ibearugbulem *et al.* (2014) and Adah (2016) as shown in Table-10 below.

Table-10 Uniaxial Buckling Load of Undeformed Rectangular Plates with Free Edge

PLATE TYPE	Ibearugbulem <i>et al.</i> (2014)	Adah <i>et al.</i> (2021)	Present Study	Percentage Difference	Percentage Difference
	N_1	N_2	N_3	$((N_3-N_1)/N_1)*100$	$((N_3-N_2)/N_2)*100$
SSFS	13.295	15.415	15.415	15.94	0
SCFS	21.547	26.472	26.472	22.85	0
CSFS	16.945	19.283	19.283	13.80	0
CCFS	27.553	21.891	29.891	8.49	0
SCFC	45.331	47.451	47.451	4.68	0
CCFC	48.376	50.714	50.714	4.83	0

Table 10 justifies the validity of the present formulation by demonstrating a close agreement between the predicted biaxial buckling loads and those reported by Ibearugbulem *et al.* (2014). The observed percentage differences, ranging from 4.83% to 22.85%, are primarily due to differences in analytical formulations and solution techniques. While Ibearugbulem *et al.* (2014) employed the Galerkin method, which relies on assumed admissible functions satisfying weighted residual conditions, the present study adopts the Ritz energy method based on total potential energy minimization. Additionally, variations in polynomial approximation order and numerical evaluation contribute to the discrepancies. Despite these methodological differences, the results exhibit consistent trends and comparable magnitudes, indicating that the proposed model reliably captures the nonlinear biaxial buckling behavior of the plates. The agreement confirms the robustness and applicability of the developed formulation, thereby validating the findings presented in this study. In addition, the comparison with the work of Adah (2016) indicates no difference at all meaning that the new model agrees with the former small deflection model. Fig. 1 shows the variations of the biaxial buckling coefficient with the biaxial buckling ratio for these plates in the undeformed state ($w/t = 0$) at an aspect ratio of 1.

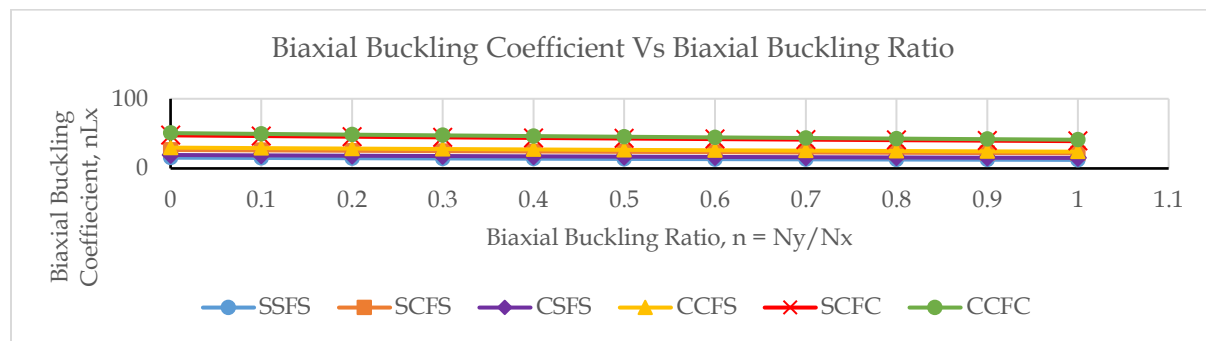


Fig. 1 Graph of Biaxial Buckling Load Coefficient vs. Biaxial Buckling Ratio for Rectangular Plates with One Free Edge and Aspect Ratio of 1.

Fig. 1 shows that the biaxial buckling coefficient decreases consistently with increasing biaxial buckling ratio for all boundary conditions. Plates with higher edge restraints, such as CCFC and SCFC, exhibit significantly greater resistance to buckling compared to less restrained plates like SSFS and CSFS. This highlights the strong influence of boundary conditions on structural stability, with clamped configurations offering the highest critical resistance under biaxial compression. Generally, the findings confirm that increasing biaxial loading reduces plate stability, with the extent of reduction governed by the plate's support conditions. This is consistent with practical behaviour of plates in particular and structures in general. To further validates the results for post buckling behaviour of plates of this nature, Figs. 2 and 3 show the comparison of the result of the uniaxial buckling load coefficient of the rectangular plates with one free edge under large deflection at an aspect ratio of 1 using the formulated equation in this study with the results of Adah *et al.* (2021).

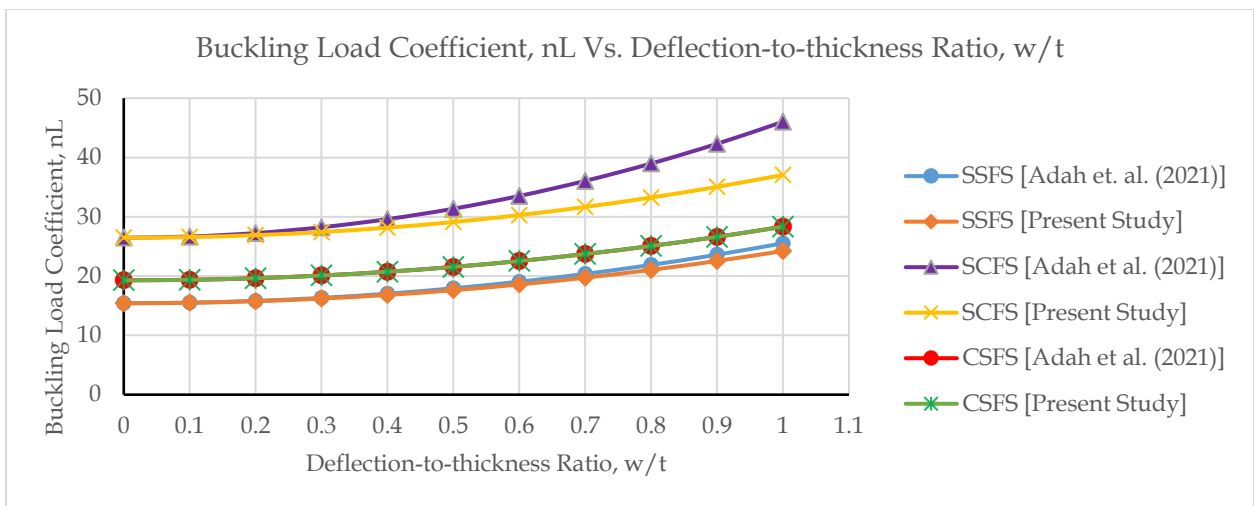


Fig. 2 Graph of Biaxial Buckling Load Coefficient vs. Deflection-to-Ratio for SSFS, SCFS, and CSFS Plates with Aspect Ratio of 1.

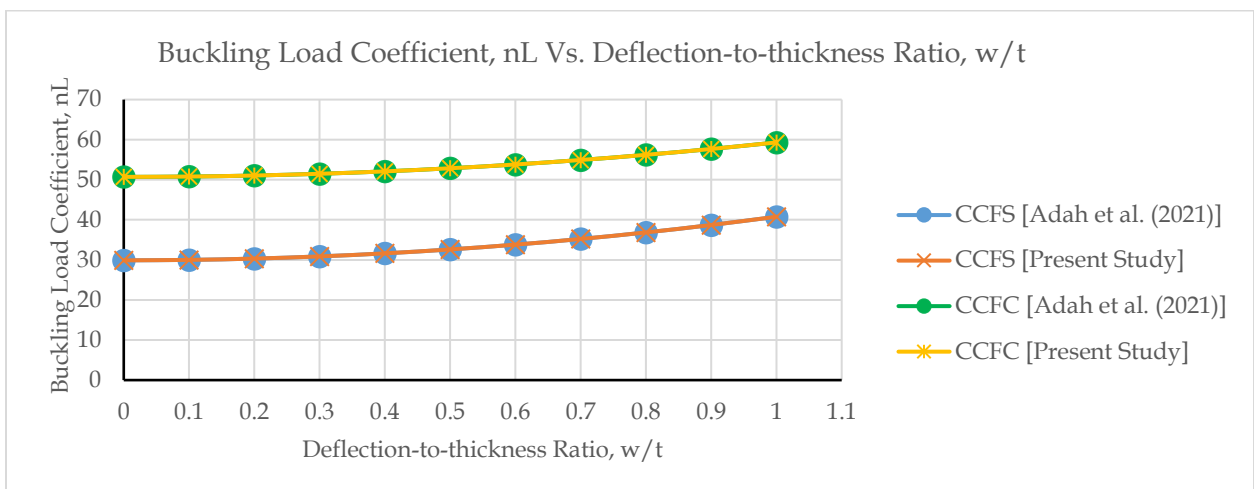


Fig. 3 Graph of Biaxial Buckling Load Coefficient vs. Deflection-to-Ratio for CCFS and CCFC Plates with Aspect Ratio of 1.

It can be observed that the uniaxial buckling load coefficients obtained in this study show excellent agreement with the results reported by Adah *et al.* (2021). For plate types CSFS, CCFS, and CCFC, the results are identical, indicating perfect consistency between both approaches. For SSFS and SCFS plates, slight deviations are observed,

with percentage differences ranging from 0% up to about 5.1% (SSFS) and 19.5% (SCFS) as the deflection-to-thickness ratio increases. These differences are attributable to variations in analytical approaches and computational approximations. Importantly, the discrepancies remain within acceptable engineering tolerance, thereby validating the accuracy and reliability of the formulated equation in this study for predicting the buckling behaviour of thin rectangular plates with free edges under large deflection. Although no existing literature provides a basis for comparison of results across varying aspect ratios and different values of the biaxial buckling ratio, n , it can be deduced that the derived model for biaxial buckling of rectangular plates with free edges under large deflection is also applicable for determining the buckling load of an undeformed thin plate subjected to uniaxial loading.

CONTRIBUTION TO KNOWLEDGE

This study contributes significantly to the field of structural mechanics by formulating a generalized nonlinear buckling model that incorporates both geometric and material nonlinearities for thin rectangular plates under biaxial compressive loading and large deflections. It derives boundary-specific buckling equations for six distinct support conditions involving a free edge, thereby improving the accuracy of buckling and post-buckling predictions. The model is versatile, accommodating various materials through parameters such as Poisson's ratio, and serves as a foundation for developing practical design tools while paving the way for future experimental validation and numerical extensions.

CONCLUSION

This paper presents a specialized buckling models developed to determine the biaxial buckling and post buckling load of thin rectangular plates with a free edge. The models demonstrate notable versatility, as it can be applied to both uniaxial and biaxial loading scenarios, accommodating cases of small and large deflection alike. Furthermore, the study provides detailed results for the biaxial buckling load coefficients of thin square and rectangular plates with free edges, specifically for configurations SSFS, SCFS, CSFS, CCFS, SCFC, and CCFC, under large deflection. The findings reveal that the biaxial buckling load coefficient of thin plates decreases as the biaxial buckling ratio increases, while a reduction in the aspect ratio leads to a corresponding decrease in the biaxial buckling ratio. Given that the results of this study align closely with those reported by [Ibearugbulem et al. \(2014\)](#) and earlier works of [Adah et al. \(2016\)](#) for the undeformed plate condition (where the deflection-to-thickness ratio, $w/t = 0$) at an aspect ratio $2 = 1$, and biaxial loading ratio $n = 0$, the additional results obtained for various combinations of n , w/t , and aspect ratios can be considered accurate and reliable. Therefore, the conclusion that the new general mathematical equation to biaxial buckling of thin rectangular plate with large deflection is applicable and suitable for the analysis of thin rectangular plates with a free edge.

CONFLICT INTEREST

There is no conflict of Interest.

SYMBOLS

These symbols are defined as;

A = Amplitude of displacement

h = shape profile of thin plate

R = Non dimensional parameter along x – direction

Q = Non dimensional parameter along x – direction

k_{bx} = Bending stiffness along x – axis

k_{bxy} = Bending stiffness along xy – axis

k_{by} = Bending stiffness along y – axis
 K_{mx} = Membrane stiffness along x – axis
 k_{mxy} = Membrane stiffness along xy – axis
 k_{my} = Membrane stiffness along y – axis
 k_{bT} = Total bending stiffness
 k_{mT} = Total membrane stiffness
 k_{Nx} = External buckling load stiffness along x – axis
 k_{Nxy} = External buckling load stiffness along y – axis
 k_{Ny} = External buckling load stiffness along xy – axis

REFERENCES

- Adah, E. I., 2016. "Development of Computer Programs for Analysis of Single Panel and Continuous Rectangular Plates" M. Eng. Thesis Federal University of Technology Owerri. (www.library.futo.edu.ng).
- Adah, E. I., Ibearugbulem, O. M., Ezeanyagu, C. F., & Okon, E. E. (2023). An Improved Formulation Of Nonlinear Strain-Displacement Relations And Specific Mathematical Models For Stability Analysis Of Thin Rectangular Plates. *Journal of Inventive Engineering and Technology (JIET)*, 3(3), 85–102.
- Altenbach, H. (2020). Plate Theory After von Kármán. *Encyclopedia of Continuum Mechanics*, 2068–2076. https://doi.org/10.1007/978-3-662-55771-6_285
- Bai, Y. (2003). *Marine structural design*. Elsevier.
- Barsotti, B. (2024). *Ship Structure Collapse Analyses Due To Nonlinear Effects, With A Focus On Cyclic Loads*. <https://tesidottorato.depositolegale.it/handle/20.500.14242/158635>
- Bilbao, S., Thomas, O., Touzé, C., & Duceschi, M. (2015). Conservative numerical methods for the Full von Kármán plate equations. *Numerical Methods for Partial Differential Equations*, 31(6), 1948–1970. <https://doi.org/10.1002/NUM.21974>
- Brighenti, R. (2005). Buckling of cracked thin-plates under tension or compression. *Thin-Walled Structures*, 43(2), 209–224. <https://doi.org/10.1016/J.TWS.2004.07.006>
- Carrera, E., Brischetto, S., & Nali, P. (2011). *Plates and shells for smart structures: classical and advanced theories for modeling and analysis* (First, Vol. 36). John Wiley & Sons.
- Chandel, V. S., Wang, G., & Talha, M. (2020). Advances in modelling and analysis of nano structures: A review. *Nanotechnology Reviews*, 9(1), 230–258. https://doi.org/10.1515/NTREV-2020-0020/ASSET/GRAPHIC/J_NTREV-2020-0020_FIG_002.JPG
- Dai, H., Yue, X., & Atluri, S. (2014). Solutions of the von Kármán plate equations by a Galerkin method, without inverting the tangent stiffness matrix. *Journal of Mechanics of Materials and Structures*, 9(2), 195–226. <https://msp.org/jomms/2014/9-2/p04.xhtml>
- Giuseppe, C., & Matteo, S. (2017). Analysis of composite beams, plates and shells. In *ICCS20-20th International Conference on Composite Structures*. Società Editrice Esculapio.
- Hassan, H. Z., & Saeed, N. M. (2024). Advancements and applications of lightweight structures: a comprehensive review. *Discover Civil Engineering* 2024 1:1, 1(1), 1–43. <https://doi.org/10.1007/S44290-024-00049-Z>
- Ibearugbulem, O., Ezech, J., & Ettu, L. (2014). *Energy Methods in Theory of Rectangular Plates (Use of Polynomial Shape Functions)*. LIU HOUSE OF EXCELLENCE VENTURES.
- Ibearugbulem, O. M., Adah, E. I., Onwuka, D. O., & Okere, C. E. (2020). Simple and Exact Approach to Post Buckling Analysis of Rectangular Plate. *International Journal of Civil Engineering*, Volume 7(6), 54–64. <https://doi.org/10.14445/23488352/IJCE-V7I6P107>

- Jerath, S. (2020). *Structural stability theory and practice: buckling of columns, beams, plates, and shells*. John Wiley & Sons.
- Jones, R. (2006). *Buckling of bars, plates, and shells*. Bull Ridge Publishing.
- Kubiak, T. (2013). Static and dynamic buckling of thin-walled plate structures. *Static and Dynamic Buckling of Thin-Walled Plate Structures*, 9783319006543, 1–188. <https://doi.org/10.1007/978-3-319-00654-3/COVER>
- Li, S., Hu, Z., & Benson, S. (2019). An analytical method to predict the buckling and collapse behaviour of plates and stiffened panels under cyclic loading. *Engineering Structures*, 199, 109627. <https://doi.org/10.1016/J.ENGSTRUCT.2019.109627>
- Megson, T. H. G. (2013). Bending of thin plates. *Aircraft Structures for Engineering Students*, 233–266. <https://doi.org/10.1016/B978-0-08-096905-3.00055-3>
- Szilard, Rudolph. (2004). *Theories and applications of plate analysis : classical, numerical, and engineering methods*. John Wiley.
- Ugural, A. C. (2017). Plates and shells: Theory and analysis. In *Plates and Shells: Theory and Analysis, Fourth Edition (Fourth)*. CRC Press. <https://doi.org/10.1201/9781315104621/PLATES-SHELLS-ANSEL-UGURAL/RIGHTS-AND-PERMISSIONS>
- Yue, Y. M., Ru, C. Q., & Xu, K. Y. (2017). Modified von Kármán equations for elastic nanoplates with surface tension and surface elasticity. *International Journal of Non-Linear Mechanics*, 88, 67–73. <https://doi.org/10.1016/J.IJNONLINMEC.2016.10.013>
- Zhang, C., & Tan, K. T. (2023). Experimental and numerical investigation of large-scale effect on buckling and post-buckling behavior of tubular structures. *Thin-Walled Structures*, 186, 110708. <https://doi.org/10.1016/J.TWS.2023.110708>
- Zhang, X., & Zhang, H. (2013). Energy absorption limit of plates in thin-walled structures under compression. *International Journal of Impact Engineering*, 57, 81–98. <https://doi.org/10.1016/J.IJIMPENG.2013.02.001>
- Zhong, X. X., & Liao, S. J. (2018). Analytic approximations of Von Kármán plate under arbitrary uniform pressure – equations in integral form. *Science China: Physics, Mechanics and Astronomy*, 61(1), 1–11. <https://doi.org/10.1007/S11433-017-9096-1/METRICS>